Low Temperature Physics/Fizika Nizkikh Temperatur, 2021, vol. 47, No. 10, pp. 949–955

Phase states and the mechanism of crystallization of condensed Ar–Kr mixtures

A. A. Solodovnik and N. S. Mysko-Krutik

B. Verkin Institute for Low Temperature Physics and Engineering of the National Academy of Sciences of Ukraine
Kharkiv 61103, Ukraine
E-mail: solodovnik@ilt.kharkov.ua

Received April 28, 2021, published online August 26, 2021

The structure characteristics of Ar–Kr mixtures deposited under special conditions have been investigated in the whole interval of concentrations applying the transmission electron diffraction technique (THEED). The samples were prepared *in situ* by condensing a gas mixture preliminary cooled down to the sub-liquid-nitrogen level onto substrates at T = 6 K and 20 K. The experimental results show that the structure and morphology of the Ar–Kr condensates are dependent on the nucleation dynamics prevailing in the course of the sample formation. It is shown that cooling a gas mixture is favorable to the clusterization of solute atoms in the gas flow. The krypton small clusters can serve as condensation clusters. The phase boundaries of the condensates have been determined. Regular Ar–Kr solutions are formed when the contents of one of the components are low (0–10 mol % Ar), (0–5 mol % Kr). The diffraction patterns of the condensates with prevailing Kr contents corresponded to a mixture of Kr-enriched fcc solutions and a dispersed phase of argon. The excess Kr contents are due to the specific morphology of the solutions dictated by condensation conditions. The Ar-based samples contained a mixture of two crystalline phases (an fcc solution and the hcp phase of nearly pure argon) and a glass phase of nearly pure krypton. In the concentration range 58–78 mol % Ar the new morphological form of the Ar–Kr condensates resembles the gel. The phase state diagram of the Ar–Kr condensates has been obtained.

Keywords: cryocondensates, structure, electron diffraction analysis, solidified inert gases, gel.

Introduction

The mixtures of solid cryocrystals attract continuous researchers' interest as model objects convenient for investigating the basic, both fundamental and applied problems of solid state physics [1–3]. In particular, they are important while developing new functional materials with pre-assigned properties, modeling glasses, gels, etc. [4]. Also, condensed systems allow a wide set of the substance states through varying the conditions of sample formation. The processes of gas phase condensation under non-equilibrium conditions are essential while solving the problems of chemistry and physics of the atmosphere, astrophysics, the Earth's climate modeling [5]. The condensation technique is widely applied to develop nanostructured materials through a special mechanism of crystallization affording the formation of nanosystems. The process of nucleation has been thoroughly investigated by the photoelectron emission method beginning with the earliest stages when free mixed Ar–Kr and Ar–Xe clusters start to form in supersonic jets [6, 7]. It is shown that the nanoaggregations of stronger-bound components (krypton and xenon in these mixtures) act as centers of heterogeneous cluster nucleation. Furthermore, there is evidence of radial segregation within the volume of Ar–Kr and Ar–Xe nanoclusters in the process of nucleation and their further growth [8, 9]. The nucleation and the growth of pure inert gas (Ar, Kr, Xe) crystals prepared by gas-phase deposition onto a substrate were investigated by electron microscopy, which is very important for checking the experimental results by comparing them with the classic nucleation theory [10].

On solving the problem of storage of energy capacitive states, a technique of preparing porous impurity-helium materials was developed to produce gels-like media [11] using inert gas atoms, nitrogen, and deuterium molecules as impurity particles forming an irregular carcass. Similar hydrogen-based structures were attempted in [12]: binary gas mixtures of normal hydrogen-krypton, hydrogen-argon atoms were condensed onto a substrate at T = 5 K. A number of experimental facts (hydrogen stabilization of an amorphous state, the temperature of cardinal system rearrangement) were analyzed in search for the possible formation

of a gel-like phase. The authors maintained that the states of their samples were in many respects similar to gels. The deposition on a cooled substrate was thought to be the main factor responsible for the formation of a gel-like phase, with no distinct reasoning being however proposed. The topical aim of this researcher is to modify the technique of forming similar states in cryocrystalline objects and to investigate their new morphological states.

The argon–krypton system is a suitable model object: it is "relatively simple" because the inert gas atoms are spherically symmetric and the particle interaction in the atomic matrix is adequately described by the Lenard-Jones potential [3]. However, the phase diagram of solid argon–krypton mixtures remained for a long time a widely debated topic and the experimental findings took on them did not agree with the thermodynamics requirements [13]. Theoretically, each particular relative concentration has its critical temperature below which a regular solid solution becomes unstable. The critical temperature of the equimolar solid argon–krypton solution is $T_{cr} = (44 \pm 3)$ K [14]. The experimental results obtained on solid Ar–Kr mixtures show no disintegration [15–17]. The investigation of diffuse and Bragg neutron scattering from polycrystalline samples at 46 K casts some doubts upon the non-limited solubility of the argon–krypton alloy [18]. We [19] have developed a technique of preparing a regular argon–krypton solution whose boundaries of equilibrium solubility, as found through an electron diffraction analysis, were 0–45 mol % Ar and 75–100 mol % Ar, the layering region being within 50–70 mol % Ar. Our results obtained on an overcooled condensed equimolar Ar–Kr mixture were somewhat unusual [20]: the equimolar cryocondensates had a multiphase morphology. It was established that the pure components and the gas mixtures exhibited different mechanisms of crystallization. This calls for further thorough structural research on overcooled condensed argon–krypton gas mixtures in the whole range of concentrations.

Experimental procedure

The structural investigations were performed by the transmission electron diffraction method (THEED) in an EG-100A electron diffractometer equipped with a helium cryostat. Observations were carried out in the temperature range from 5 K to the krypton sublimation point (44 K). The electron diffraction technique is detailed in [21]. Here we point out the important features of the study. The cryostat cryoscreens were designed to allow temperature variations of the path feeding the gas mixture onto a film substrate within the room–sub-LN (slightly below the liquid-nitrogen point) interval temperature, which afforded broad-range conditions of sample condensation. To ensure reliable cooling, the gas puffing rate was rather low, typically no more than 10^{-4} cm^3/s, which corresponds to the deposition rate of 2–3 A/s. The gas mixtures cooled to the sub-liquid nitrogen temperature (indicated as sub-LN) were condensed on composite film substrate which consisted of polycrystalline aluminum and compatible amorphous carbon. Aluminum was used as a standard for determining the lattice parameter while the carbon was helpful in the analysis of the diffraction maxima intensities. The lattice parameter measurement accuracy was not worse than ± 0.005 Å. The relative intensity error was 7–10 %. The argon and krypton gases used were 99.98 % pure. The gases were mixed in a special vessel and kept at room temperature to attain their uniform distribution. The net pressure in the bottle did not exceed 12 Torr. The mixture compositions were determined by a difference between the partial pressures of the components. The samples were prepared *in situ* in a cryostat at substrate temperatures of (T_{dep}) 6 K or 20 K. The temperature error being no more than ± 0.25 K. The electron diffraction patterns were obtained at (T_{sample}) 6 K or 20 K. These experimental conditions (gas mixture temperature, puffing rate, substrate temperature) led to the formation of condensates whose properties and morphology differ drastically from regular solutions [22, 23]. The electron diffraction patterns were taken directly after sample preparation at the pre-assigned temperature and in the process of their further heating to the required temperature. The duly developed patterns were digitized using a CanoScan9950F scanner with the resolution 1200 dpi, the maximum optical density of the scanner being 3.8 D. The further computation was performed using the ImageJ, Origin, and MathCad packages.

Results and discussion

The experimental Ar–Kr condensates obtained by depositing overcooled (sub-LN) gas mixtures at 20 and 6 K were polycrystalline samples. To analyze the diffraction patterns, the concentration interval was separated into portions, each holding a prevailing content of one of the components, and a close-to-equimolar region. The structure of the samples and its features were determined. It is reasonable to consider the experimental results starting with the analysis of the structures and their features.

Krypton-based condensates (*the gas phase composition is 0–47 mol* % Ar)

The obtained diffraction patterns of solidified Ar–Kr mixtures comply with the single reflection system. According to the calculation, the reflections correspond to the fcc phase (see Table 1). The typical electron diffraction pattern is shown in Fig. 1(a). Its intensity distribution is seen to fit

Table 1. The interplanar distances in Kr–5.9 mol % Ar condensates. T_{dep} =20 K, T_{sample} = 20 K

hkl	*d*, Å^{-1}
111	3.262
200	2.858
311	1.707
222	1.643

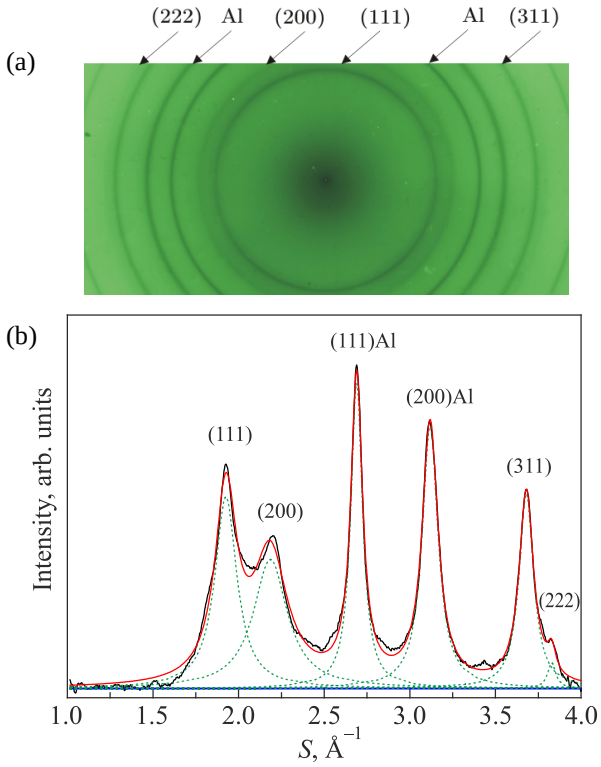

Fig. 1. (a) The densitogram of Kr–5.9 mol % Ar condensate. T_{dep} = 20 K, T_{sample} = 20 K. (b) The electron diffraction pattern of the Kr – 5.9 mol % Ar condensate. T_{dep} = 20 K, T_{sample} = 20 K. The dotted curve — the Lorentz function approximation.

well within the description of the cubic modification. The geometry of the electron diffraction patterns was calculated and the analysis of the diffraction maxima shapes was performed. The subtraction of the incoherent scattering and the Gauss–Lorentz approximation of the diffraction reflection disclosed a minimum discrepancy between the experimental and model curves (about 7 % after the Lorentz function approximation). The results obtained are shown in Fig. 1(a): the densitogram corresponds to the electron diffraction pattern (Fig. 1(b): experiment — solid curve, the Lorentz function — dotted curve).

The analysis of the intensity distribution in the concentration interval 0–47 mol % Ar revealed no additional phases. The features of the condensate structure and morphology can be found out from the behavior of the lattice parameters as a function of the composition. The results measured on the fcc phase are shown in Fig. 2: shaded squares — experiment, dash-and-dot line — Vegard-rule calculation, dashed line — Prigogine-theory calculation.

It is known that the lattice parameter of a solid mixture is independent of its composition, which, among other factors, suggests no solution formation. In our samples with dominant Kr contents the lattice parameters were observed to decrease gradually in the concentration interval 0–40 mol % Ar. The monotonous change in the lattice parameter dependence points to certain solubility of the components and the formation of a solid solution. With low argon contents

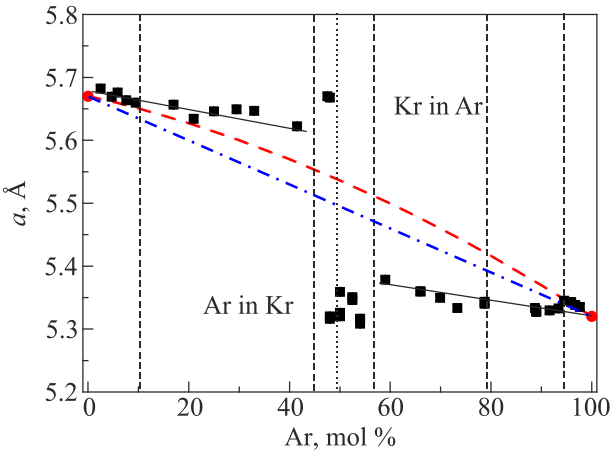

Fig. 2. The lattice parameters *a*: the fcc phase of the Ar–Kr condensates as a function of the composition. T_{dep} = 20 K, T_{sample} = 20 K, experimental results (■), Vegard rule-based calculation (dash-and-dot line), Prigogine theory calculation (dashed line).

(up to 10 mol % Ar) the experimental dependence of the lattice parameters obeys the Vegards rule and agrees with Prigogine theory. This dependence is similar to that obtained for regular Ar–Kr solutions [19]. It is possible that overcooling of a mixture with low impurity additives does not influence the crystallization mechanism, just like in the case of pure components. We showed [20] that the structures of pure argon and krypton are independent of the gas temperature. This was evident while preparing a "sandwich" sample in which the layers of sub-LN pure argon and krypton were condensed onto a substrate by stages. In this case, the diffraction pattern showed overlapping of the argon and krypton fcc lattices with no peculiar features. As the Ar contents in the gas mixture grow further, the experimental lattice parameters start to exceed the calculated ones and such deviation increases with approaching the pre-equimolar region. The true contents of argon in the condensate was not higher than 12 mol %, its portion in the gas mixture being 41 mol % Ar. The weak correlation between the lattice parameters of argon–krypton condensates and the starting gas mixture compositions may be due to the discrepancy between the component concentrations in the sample and the mixture or some other factors. Deficient condensation of a part of argon onto a substrate is prohibited by the energy conditions: the melting temperature of argon is 83.78 K below that of krypton (T_m = 115 K) [1, 2]. The excess concentration of one of the mixture components may be attributed to a specific morphology caused by the redistribution of impurity atoms. We may thus assume that the observed effect of enrichment with the higher binding-energy component is induced by the processes occurring while overcooling the gas mixture. It is known that the binding energy in krypton (0.116 eV) is almost 1.5 times higher than that in argon (0.08 eV) [24]. On cooling the gas mixture, small (one or two krypton aggregations of one or two atoms) start to form and then grow into larger clusters.

Thus, the first stage of nucleation develops in the gas flow. Since argon is a surface-active to krypton, the krypton nanoaggregations can contain argon atoms. The argon that remains outside the solution lattice forms a fine-disperse fraction on the substrate. None of these crystallites is capable of forming detectable coherent reflexes. The character of the recrystallization process which decreases the noncoherent background of the electron diffraction patterns above the sublimation temperature of argon is indirect evidence of the presence of argon "coat" on the substrate. The condensation of Kr–based sub-Ln gas mixtures leads to the formation of a solid substitution solution in the concentration range 0–10 mol % Ar. The specific- morphology Ar–Kr condensates and Ar "coat" are formed due to the changes in the nucleation mechanism in the region 10–47 mol % Ar.

As the gas mixture approaches the equimolar composition ($\geq$ 48 mol % Ar), the morphology of the samples changes sharply, which is clearly seen in the electron diffraction patterns: the reflections of the solid solution phase disappear and a distinct diffraction pattern appears, which corresponds to the fcc phase of pure argon and pure krypton (see Fig. 3), the lattice parameters being a(Kr) = 5.667 Å and a(Ar) = 5.316 Å. This means that increasing Ar contents bring the condensate to decompose into the starting pure components, which is not typical of the classical case. It is known that layering of a regular solution produces solid solutions of ultimate permissible concentrations. The decomposition process provides good supporting evidence for the unusual morphology of condensed sub-LN argon–krypton mixtures with a predominant Kr content. This type of decomposition was investigated theoretically on binary inert gas clusters [25]. The segregation into pure components was observed only in free heterogeneous argon–xenon clusters [26] whose structures correspond to the xenon core within an argon shell. The changes in the condensate structure and morphology attest to the specific features of the phase that develops under extreme non-equilibrium conditions of crystallization.

Argon-based condensates (*gas phase composition of 55–100 mol %* Ar)

The samples were prepared by depositing sub-LN Ar–Kr gas mixtures onto substrates at 20 K and 6 K. Their electron diffraction patterns corresponded to those of polycrystalline samples. Reasoning from the maxima positions the set of diffraction reflections can be described within the cubic lattice. At concentrations close to that of pure argon (up to 5 mol % Kr) the sample structures correspond to the fcc lattice. As the krypton contents grow, the diffraction patterns exhibit a number of intensity distribution features. The typical densitogram for Kr + 94 mol % Ar sample is shown in Fig. 4: reflection (111) is asymmetric and broadens on the left-hand side; the peak (200) is strongly smeared and overlaps with maximum (111), which produces bending of its right-hand arm. The anomalies are most pronounced in the interval of diffraction vectors S = 1.8–2.25 Å^{-1}. The analysis of the diffraction reflection shapes and the Lorentz function approximation of the intensity distribution curve have revealed additional reflections related to the fcc phase, which prohibits the monophase description of the samples. It is also found that the left-hand wing of peak (111) has a reflection whose position corresponds to S = 1.95 Å^{-1} while reflection (111) itself is strengthened with a maximum in the region S = 2.056 Å^{-1}, and the right-hand side has a reflection at S = 2.34 Å^{-1}. These reflections were indexed as (001), (002), and (101) of the hcp phase and the hcp lattice parameters were calculated: a = 3.741 Å, c = 6.112 Å, c/a = 1.6337.

The hcp phase reflection (102) is overlapped by the reflection (111) from the aluminum standard. The identification of the hcp modification is quite unambiguous: the hexagonal phase presents in the argon-based samples. It is known that the stability of the cubic structure in inert gas crystals can be broken by various factors including impurities. As structural investigations [27] show, molecular impurities can stabilize the hcp phase in argon. However, the ef-

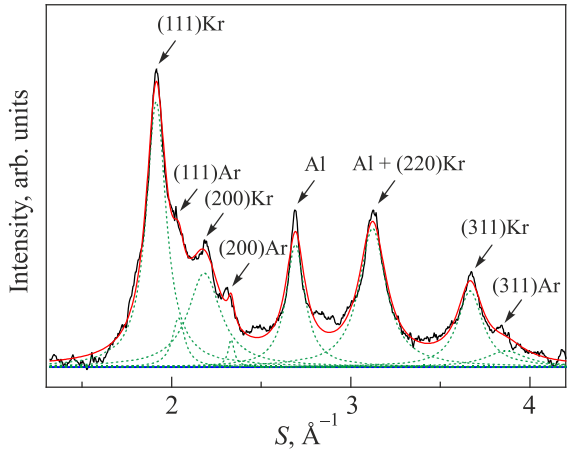

Fig. 3. The diffraction pattern of the Kr–48 mol % Ar condensate. T_{dep} = 20 K, T_{sample} = 20 K.

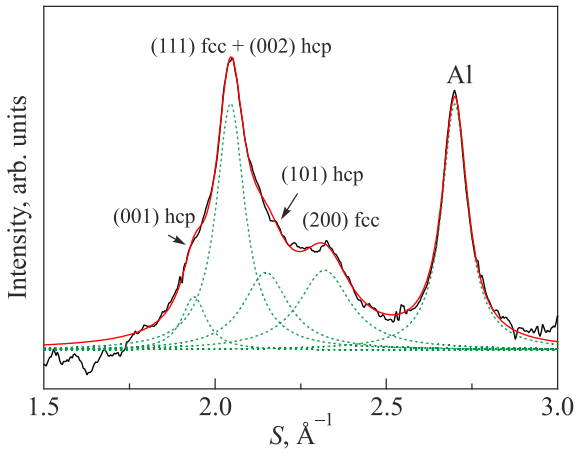

Fig. 4. The diffraction pattern of the Kr–94 mol % Ar condensate. T_{dep} = 20 K, T_{sample} = 20 K.

fect of atomic krypton on the fcc–hcp transition in the condensed state has been revealed for the first time in this study which was favored by the special conditions of condensation. The coexistence of hcp and fcc phases in the condensed state was observed while investigating free Ar–Kr clusters [28]. The presence of the fcc and hcp phases does not suggest the "standard decomposition" of a solid solution because both the phases have almost identical molar volumes (V_{fcc} = 22.586 cm^3/mol, V_{hcp} = 23.59 cm^3/mol). However, the volumes of solid Ar- and Kr-based phases are expected to be about 12 % different. On layering, the classical binary solid solution forms monosolutions based on either of the components of maximum permissible concentration. Thus, the cubic and hexagonal phases are crystalline modifications of solid Ar-based solutions. The difference in energy between the cubic and hexagonal lattices is quite small for inert gas crystals.

The approximation of the densitometric curve in the concentration range 50–70 mol % Ar has revealed a halo and a system of reflections in the small-angle region. The typical diffraction pattern is shown in Fig. 5. The halo position and half-width are practically independent of the sample temperature. The experimental findings show that the condensates have a multi-phase morphology, i.e., crystalline and disperse phases can coexist. Also, liquid-like formations appearing along with the fcc and hcp modifications were observed in experiments on large free Kr doped with Ar clusters [29]. The fact was interpreted as nonclassical properties of clusters. Note that nucleation starts when the temperature in the Ar–Kr mixture jets is about 60 K [6], which is close to the experimental conditions of condensing gas mixtures in this study.

The revealed coexistence of two crystalline modifications brings up the question: what effect does the concentration dependence have upon the content correlation of the two phases (hexagonal and cubic) in the sample. It is known that the diffraction intensity is proportional to the scattering volume), which allows estimation of the variations in the hcp/fcc composition. The phase correlation was analyzed through plotting a relationship between the integral intensities of the reflections unambiguously belonging to different phases: reflections (101) hcp and (200) fcc. The ratios I_{100}/I_{200} calculated as a function of composition are shown in Fig. 6. It is seen that the relative quantity of the hexagonal fraction increases with the krypton concentration up to the maximum value in the equimolar region, which may be due to the static stress in the lattice. The structural characteristics of the hexagonal modification were practically independent of the sample composition (c = 6.12 Å; a = 3.75 Å; c/a = 1.633).

The lattice parameters of the cubic phase of Ar-based condensates have been investigated (see the measurement results in Fig. 2). The experimental points obtained for a single-phase solution (95–100 mol % Ar) are close to the Vegard rule and Prigogine theory calculations. This fact indicates the formation of a solid substitution solution. Note that the composition of the condensate corresponds to that of the deposited gas mixture. On a further increase of the Kr contents in the gas mixture, the fcc lattice parameters depart from the calculated curves towards lower values. The observed weak concentration dependence of the lattice parameters suggests the formation of a solid solution. The highest krypton contents in the solution are no more than 10 mol %. The discrepancy between the compositions of the condensate and the starting gas mixture and the slower growth of the lattice parameter of the solid solution may be attributed to the specific morphology and the presence of Kr in the disperse phase. The presence of krypton on the substrate is undoubtedly supported by the specific procedure of sample annealing: after Ar sublimation above T = 32–33 K the halo transformed into a diffraction pattern of crystalline krypton. It should be noted that a part of Ar atoms are also involved in the formation of the halo (see our results for equimolar Ar–Kr gas mixtures in [20]).

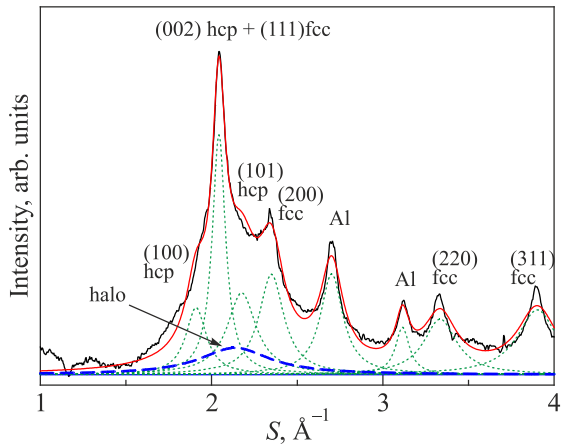

Fig. 5. (Color online) The diffraction pattern of the Kr–70 mol % Ar sample. T_{dep} = 20 K, T_{sample} = 20 K. The dotted curve — the Lorenz-function approximation, the dashed curve — halo, the black curve — experimental values.

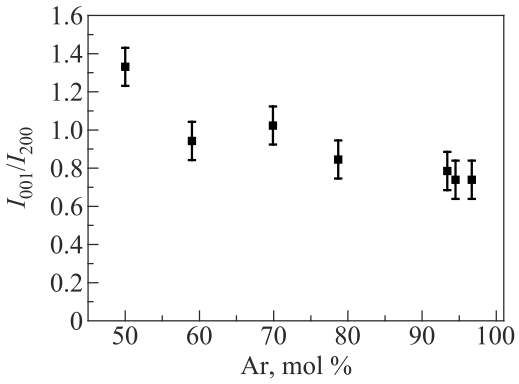

Fig. 6. The concentration dependence of the intensity ratio between the hcp reflection (001) and the fcc maximum (200) as an illustration of a change in the partial contributions of these structures.

When the Kr contents in the gas mixture exceed 40 mol %, the fcc solution disintegrates. The resulting condensate structures have a cubic and hexagonal of argon and the disperse Krypton phase.

On annealing low temperature (T_K = 6 K) multiphase condensates the disperse and fcc phases were insensitive to heating. The heating to T = 20 K had little or no effect on the sizes of the fcc crystallites up to the point of Ar sublimation. In the course of annealing, the reflections of the hcp phase became more distinct and the coherent regions scattering increased by a third (from 75 to 110 Å). The temperature transformation of the halo (T > 33 K) is caused by Ar sublimation: the center of the halo shifts towards smaller angles and its half-width decreases. However, without argon, this is already a krypton sample. The thermal stability of the two phases may be attributed to the amorphous matrix which seals off the grains of the solid solution and thus prohibits their growth. This recrystallization pattern is similar to what is observed on annealing gels: they also remain insensitive to heating up to a certain temperature. It is then safe to assume that the state discussed above is morphologically a gel-like phase.

The results obtained provide a qualitative picture of the morphology and phase boundaries for argon–krypton condensates in the whole interval of concentrations (see the phase states diagram in Fig. 7).

The phases of unusual morphology observed in the atomic Ar–Kr system are due to some “non-classical” mechanism of nucleation. In this study, the cooling of a gas mixture to sub-liquid-nitrogen temperatures favors the formation of nanoparticles which are conducive to nucleation in the course of condensate formation. A part of argon atoms can be bonded to krypton particles. The “non-classical” mechanism of nucleation is basic to the formation of Ar–Kr condensates of unusual morphology. The “structural subtlety” of the decomposition process in regular Ar–Kr solutions can be attributed to various nucleation mechanisms that become active during the formation of solid solutions. This can well account for the discord in experimental data in the literature.

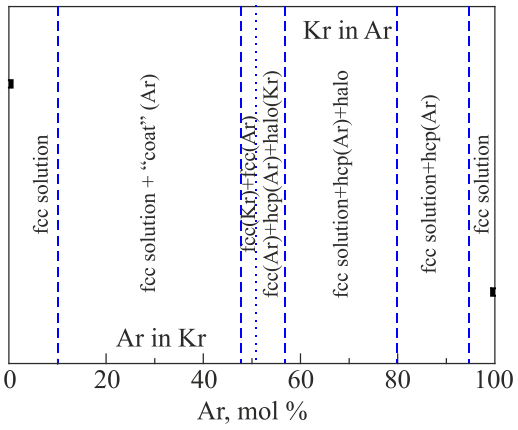

Fig. 7. The phase state diagram of the Ar–Kr condensates as a function of the composition. T_{dep} = 20 K, T_{sample} = 20 K.

Conclusions

The structure and morphology of Ar–Kr condensates deposited at high-degree overcooling of gas mixtures have been investigated in the whole concentration range of both components. The data reported were obtained through a thorough analysis of the sample structures, the dependences of the lattice parameters upon the sample composition, the diffraction reflection profiles, and also the phase composition of the samples.

A regular Ar–Kr solution was formed in solid mixtures with low contents of one of the components (0–10 mol % Ar and 0–5 mol % Kr).

The condensates with prevailing Ar contents were found to have three coexisting phases: two crystalline phases formed mainly of argon and a disperse phase consisting predominantly of krypton. One of the crystalline argon phases was structurally a solid solution with a fcc lattice while the other was made up of almost pure argon of hexagonal modification. Also, the conditions were realized when the largest part of one of the components formed crystalline phases while the largest part of the other component built up a glassy state. The analysis of the morphology and the recrystallization process performed on the samples of 58–78 mol % Ar led us to reveal the formation of a gel-like state.

The formation of a fcc solution enriched in krypton was observed in the concentration region 10–48 mol % Ar. In this case, a large part of argon exists as a phase producing no coherent scattering.

The sample morphology changes drastically in the narrow pre-equimolar region (48–50 mol % Ar), which is due to a non-classical decomposition of the solid solution into pure components.

It has been found that the structure and morphology of sub-LN Ar–Kr condensates are strongly dependent on the nucleation dynamics prevailing in the course of sample formation. It is shown that bringing the temperature of the gas mixture deposition to the sub-LN level is favorable for nucleation in the gas flow. Here is how a “non-classical” two-step process of nucleation develops in which krypton nanoparticles are of basic importance.

This is for the first time that morphologically different types of condensates have been obtained in the atomic Ar–Kr system. The presented experimental results (except those for the regions of low contents of the components) cannot be described within the theory of regular solutions. The facts outlined are brought out here to generate interest in further theoretical research.

1. B. I. Verkin, A. F. Prikhotko, V. G. Manzhelii, I. Ya. Fugol, Yu. B. Gaididei, I. N. Krupsskii, V. M. Loktev, E. V. Savchenko, V. A. Slysarev, M. A. Strzhemechnyi, Yu. A. Freiman, and L. I. Shanskii, *Cryocrystals*, Naukova Dumka, Kiev (1983) [in Russian].

2. V. G. Manzhelii and Yu. A. Freiman, *Physics of Cryocrystals*, New York: AIP Press (1997).
3. *Rare Gas Solids*, M. L. Klein and J. A. Venables (eds.), Academic Press, London (1976), Vol. 1; (1977), Vol. 2.
4. C. P. Poole, Jr. and F. J. Owens, *Introduction to Nano-Technology*, John Wiley & Sons, Hoboken, New Jersey (2003).
5. O. Hellmuth, V. I. Khvorostyanov, J. A. Curry, A. K. Shchekin, J. Schmelzer, R. Feistel, Y. S. Djikaev, and V. G. Baidakov, *Nucleation Theory and Applications*, Joint Institute for Nuclear Research, Dubna (2013).
6. Yu. S. Doronin, E. A. Bondarenko, and V. N. Samovarov, *Fiz. Nizk. Temp.* **32**, 337 (2006) [*Low Temp. Phys.* **32**, 251 (2006)].
7. M. Lundwall, M. Tchaplygin, and G. Ohrwall, *Chem. Phys. Lett.* **392**, 433 (2004).
8. M. Tchaplyguine, M. Lundwall, M. Gisselbrecht, G. Öhrwall, R. Feifel, S. Sorensen, S. Svensson, N. Mårtensson, and O. Björneholm, *Phys. Rev. A* **69**, 031201(R) (2004).
9. Yu. S. Doronin and V. N. Samovarov, *Opt. Spectrosc.* **102**, 906 (2007).
10. J. A. Venables, *Proc. R. Soc. Lond.* **A322**, 331 (1971).
11. S. I. Kiselev, V. V. Khmelenko, D. M. Lee, V. Kiryukhin, R. E. Boltnev, E. B. Gordon, and B. Keimer, *Phys. Rev. B* **65**, 024517 (2001).
12. M. A. Strzhemechny, N. N. Galtsov, and A. I. Prokhvatilov, *Fiz. Nizk. Temp.* **29**, 522 (2003) [*Low Temp. Phys.* **29**, 699 (2003)].
13. I. Prigogine, *The Molecular Theory of Solutions*, North-Holland, Amsterdam (1957).
14. B. E. Fender and G. D. Halsey, *J. Chem. Phys.* **42**, 127 (1965).
15. B. F. Figgins, *Proc. Phys. Soc.* **72**, 732 (1960).
16. A. E. Curzon and A. J. Mascall, *J. Phys. C* **2**, 220 (1969).
17. S. I. Kovalenko, E. I. Indan, and A. A. Khudoteplaya, *Phys. Status Solidi A* **13**, 235 (1972).
18. H. M. Gilder, *Phys. Rev. Lett.* **61**, 2233 (1988).
19. A. A. Solodovnik and N. S. Mysko-Krutik, *Fiz. Nizk. Temp.* **45**, 637 (2019) [*Low Temp. Phys.* **45**, 545 (2019)].
20. V. V. Danchuk, A. A. Solodovnik, N. S. Mysko, and M. A. Strzhemechny, *Fiz. Nizk. Temp.* **41**, 546 (2015) [*Low Temp. Phys.* **41**, 424 (2015)].
21. A. A. Solodovnik, V. V. Danchuk, and N. S. Mysko, *Fiz. Nizk. Temp.* **39**, 586 (2013) [*Low Temp. Phys.* **39**, 456 (2013)].
22. J. H. Hildebrand and R. L. Scott, *Regular Solutions*, Hardcover, Import (1962).
23. E. A. Guggenheim, *Mixtures: The Theory of the Equilibrium Properties of Some Simple Classes of Mixtures Solutions and Alloys*, Clarendon Press, Oxford (1952).
24. C. Kittel, *Introduction to Solid State Physics*, Wiley, New York (1953).
25. A. S. Clarke, R. Kapral, and G. N. Patey, *J. Chem. Phys.* **101**, 2432 (1994).
26. O. G. Danylchenko, Yu. S. Doronin, S. I. Kovalenko, and V. N. Samovarov, *JETP Lett.* **84**, 324 (2006).
27. C. S. Barrett and L. Meyer, *J. Chem. Phys.* **42**, 107 (1965).
28. O. G. Danylchenko, S. I. Kovalenko, O. P. Konotop, and V. N. Samovarov, *Fiz. Nizk. Temp.* **40**, 1391 (2014) [*Low Temp. Phys.* **40**, 1083 (2014)].
29. A. G. Danylchenko, S. I. Kovalenko, and V. N. Samovarov, *Fiz. Nizk. Temp.* **34**, 1308 (2008) [*Low Temp. Phys.* **34**, 1030 (2008)].

Фазовий склад та механізм кристалізації конденсованих Ar–Kr сумішей

A. A. Solodovnik, N. S. Mysko-Krutik

Структурні характеристики сумішей Ar–Kr, осаджених в особливих умовах, досліджено методом трансмісійної електронографії (THEED) у всьому інтервалі концентрацій. Зразки готувались *in situ* конденсацією газової суміші, що охолоджена до субазотного рівня, на підкладку при температурах 6 та 20 K. На основі експериментальних результатів було встановлено, що структура та морфологія Ar–Kr кріоконденсатів залежать від динаміки нуклеації, що переважає при формуванні зразків. Показано, що охолодження газової суміші сприяє кластеризації одиничних атомів у газовому потоці. Визначено фазові межі конденсатів. При малому складі одного з компонентів (0–10 мол % Ar), (0–5 мол % Kr) формуються регулярні Ar–Kr розчини. Дифракційні картини конденсатів з переважним складом криптону відповідали суміші ГЦК розчинів, які збагачено криптоном, та дисперсній фазі аргону. Встановлено, що в зразках на основі аргону міститься суміш двох кристалічних фаз (ГЦК розчин та ГЩУ фаза майже чистого аргону), а також скляна фаза майже чистого криптону. Нова морфологічна форма Ar–Kr конденсатів подібна до гелєвих станів. Визначено діаграму фазових станів конденсатів Ar–Kr.

Ключові слова: кріоконденсати, структура, електронографія, затверділі інертні гази, гель.